Using Analytical Force Model for Efficient Deformation Simulation and Haptic Rendering of Soft Objects

Xue-Jian He, Kup-Sze Choi
Centre for Integrative Digital Health, School of Nursing
The Hong Kong Polytechnic University
Hong Kong, China

Abstract

High refresh rate required for haptic rendering has been an issue in immersive virtual-reality based simulation. It prohibits the use of physically accurate yet computationally intensive force models. In the paper, we propose to adopt analytical force model to render feedback forces during interactive simulation of soft-object deformation, which allows force computation to be executed directly in the 1 kHz haptic servo loop. The force model is explicitly expressed by the size and shape of tool-tip and the physical properties of materials. On the other hand, graphics rendering of the resulted deformation is achieved with efficient geometric modeling, where the size of the deformed region is calibrated with simulated deformation calculated using the finite element method (FEM) to guarantee physical accuracy. Experimental results demonstrate that the forces rendered by the analytical force model are comparable to that of FEM simulation. The proposed approach has the potential to be an alternative approach to interactive deformation simulation of soft objects in virtual reality applications.

Keywords: deformation simulation, soft object, analytical force model, haptic rendering.

1. Introduction

Studies of interactive deformable models with haptic feedback have been reported extensively in the literature [1-5]. The applications include cloth simulation, animal and human character modeling, facial expressions, medical image-analysis and medical simulation. In medical simulations, the feedback forces are replicated based on the behavior of human tissues and have to be updated at high refresh rate on the

order of 1 kHz to maintain stable haptic feeling. Realistic physics-based models such as the conventional finite element method (FEM) are often very complex and requires high computational power, and therefore not suitable for real-time haptic rendering. The situation is further exacerbated when graphics rendering of deformation is also required, even simple deformation models such as mass-spring system (MSS) could also be computationally too expensive for real-time simulation, let alone the conventional FEM. Consequently, deformable simulation with haptic interactions remains a challenge.

Modeling and interactive simulation of soft-object deformation have been widely studied in computer graphics [2,6]. Many techniques have been proposed and they can be broadly classified into two categories: the non-physics-based models and physics-based models. Non-physics based models are derived from geometric modeling algorithms to present deformed objects in a visually-plausible fashion. Typical approaches include deformable spline surfaces [7 ,8], free form deformation [9] and space warping [10]. Although physical behavior could possibly be simulated by incorporating elastic properties directly into the geometrical models [7], it remains a difficulty for these methods to replicate actual mechanical response during interactive deformations. Hence, the non-physics based method are usually used in applications where physical loyalty is not a main concern [11], e.g. computer animation and computer-aided design, rather than medical simulation.

For physics-based models, FEM and MSS are the two main schools of approaches. In FEM, deformable object is partitioned into a collection of small elements, conventionally in the form of tetrahedrons. The equations of motion are then derived for each element as a function of the nodal displacements of the tetrahedrons, resulting in a discretized model in the spatial domain. A major problem with FEM-based approaches in real-time haptic rendering of soft-object deformations is the intensive computation involved, which must be completed typically within 1 ms for every update [5]. In MSS, soft object is modeled as discrete mass points linked by springs and dampers. Like FEM, the dynamic behaviors of the object are simulated by applying Newtonian mechanics to the mass points. Further details can be found in [12]. Compared to FEM, it is relatively simple to implement and convenient to handle topological changes. However, MSS models have some intrinsic disadvantages, e.g. incapability of rapid global propagation of deformation and difficulty in maintaining constant volume [2]. Another much criticized

aspect is that MSS models do not allow accurate modeling of material properties since the model parameters are usually adjusted manually or only determined by heuristic methods. As a result, interactive deformation simulation is in general a trade-off between computational time and modeling accuracy.

In this paper, we aim to develop an efficient approach for interactive deformable-object simulation that produces both realistic visual effect and high-fidelity force feedback. As high haptic refresh rate is the main hurdle, we propose to use an analytical force model to expedite force rendering. Here, we focus on haptic interactions between a soft object and a pen-like tool with tool base (i.e. tool-tip) of different shapes. The tip size is assumed to be relatively small compared to the soft object so that the interactions can be considered as contacts with an elastic plane, and therefore the forces can then be explicitly computed using the contact theory. The validity of this approach will be studied by investigating the effect of the object's surface curvature on the accuracy of simulated forces. On the other hand, to avoid intensive computations, surface deformations due to tool-object interactions are modeled geometrically in real time. The object's surface, represented parametrically by Bézier surface meshes, is deformed interactively depending on the amount of indentation by the tool. To guarantee physical accuracy, the extent of deformation is calibrated with the simulation results obtained using FEM.

The rest of the paper is organized as follows. First, related work about physics-based models of soft-object deformations is reviewed in section 2. The analytical force model and the rendering of surface deformations are discussed in section 3. The timing performance and the accuracy of the feedback forces of the proposed approach are evaluated with experiments in section 4. Discussions and conclusions are given in section 5 and 6 respectively.

2. Related Work

Considerable research efforts have been dedicated to efficient and stable haptic rendering, including god object [13], proxy [14], virtual coupling [15], multi-rate [16], voxel sampling [17], SQ-Map [18], to name a few. However, in this section, only the studies related to soft-object deformations for medical simulation using haptic interfaces are discussed. To realize physics-based simulations, parametric methods and data-driven methods have been proposed to model soft deformable objects [11]. Parametric

methods define an explicit model with a set of parameters that control the behavior of the object. MSS models are the most popular parametric method. As mentioned previously, it is simple to implement a MSS model and topological changes due to deformations can be handled easily. In addition, the computation is fast and can be readily accelerated by parallel computing techniques via graphics processing unit (GPU) [3,19]. However, conventional MSS models usually rely on heuristic methods to determine the model parameters, thus not allowing accurate modeling of the material properties. While a recent work has shown that a MSS model can be parameterized using hyper-elastic constitutive laws [20], but the accuracy of the model cannot be validated easily.

More accurate physics-based models have been developed based on continuum mechanics such as FEM [21-23]. Conventional FEM is computationally demanding and many studies have been conducted to reduce the computation overhead for interactive simulations. For example, small displacements are assumed in the application of FEM for modeling soft-object deformations [21]. Pre-computation of deformation responses is also used to effectively increase computation speed to achieve both real-time deformations and haptic feedback. For large and rotational deformations, co-rotational methods are required to avoid inflation artifacts caused by inaccurate force modeling [22]. Besides, explicit integration scheme [23] and hardware acceleration using GPU [24] are also employed to achieve real-time soft-tissue deformations using FEM.

On the other hand, data-driven methods simulate the behaviors of deformable objects based on actual measurements of mechanical responses made on the real objects, or data pre-computed offline using computational algorithms. The data are then retrieved to generate the visual and kinesthetic responses of virtual deformable objects in real time. The methods have been developed in recent years to overcome the issues with parametric methods, i.e., the difficulty to achieve real-time performance particularly in demanding real-time applications such as haptic rendering, and problems in modeling complex objects and nonlinear material behaviors [1,25,26]. For example, Pai et al. [1] developed a deformation simulation method using linear elasto-static models by measuring the mechanical responses of a real deformable object. In this method, the stiffness matrix of the FEM model was estimated using the experimental data. Furthermore, neural network techniques were adopted to reduce the number of the sampling points in the

measurement [26]. Data-driven models are however limited by experimental settings, due to that the measured data cannot be re-used and generalized for the objects with different geometry or physical properties. They are therefore not as flexible as their parametric counterparts [11].

3. The Simulation Framework

The key idea of the proposed simulation method is to expedite haptic rendering by employing an analytical force model to generate feedback forces in response to tool-object interactions. In addition, to speed up graphics rendering, the deformation of the soft object is visually rendered by locally changing the shape of the object's surface mesh in real time in response to the amount of indentation made by the tool. The undeformed region is not updated. There are two issues here. First, since the analytical force model to be adopted only concerns deformations of a plane by the tool-tip, it is necessary to evaluate its applicability in general to the deformations of curved surfaces. Second, as the deformations of surface meshes are only modeled geometrically, it is also necessary to determine, using a physics-based method, the size of the deformed region when the mesh is indented to different extents, so that the shape of the deformed mesh can be modified accordingly to visually display the deformations in a realistic manner. To tackle these issues, an offline FEM simulation is performed to obtain benchmarking data for verification and calibration as shown in Fig. 1. The FEM model is used as a benchmark to calibrate the proposed analytical model. It only serves as a benchmark to tune and evaluate the accuracy. Even so, there are still errors between the FEM model and the proposed model, while the latter can achieve a good trade-off between accuracy and computation speed. The offline FEM simulation determines and provides the relationship between insertion depth (δ) and surface deformation size (R_d). Based on this result, a mesh deformation model is developed to render the deformed surfaces. The insertion depth is also fed into the analytical force model, wherein the insertion force is calculated. Then, a resistant force is generated and sent to the haptic interface.

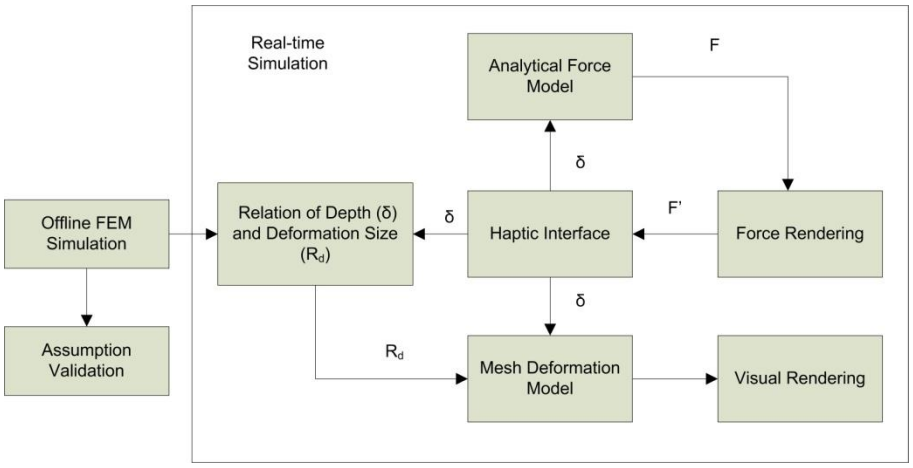

Fig. 1. Workflow of the analytical force model.

3.1 **Analytical Force Model**

Refer to Fig. 2(a), for a rigid tool whose base is geometrically described by a function φ, if it is loaded by a vertically and centrally applied force F and pushed to depress against a horizontal and isotropic elastic half plane, the indentation force can be expressed generally by the function

$$F = \emptyset(\varphi, \delta, E, v) \tag{1}$$

where δ is the vertical displacement of the tool, E is Young's modulus and v is Poisson ratio. When a tool with a spherical base of radius R is used, for a small deformation, the radius r of the circular contact area and the vertical displacement can be explicitly expressed as [27]

$$\boldsymbol{r} = \left[\frac{\mathbf{3}(\mathbf{1}-\boldsymbol{v})\boldsymbol{FR}}{\mathbf{8}\boldsymbol{G}}\right]^{\mathbf{1}/\mathbf{3}} \quad \text{and} \tag{2}$$

$$\boldsymbol{\delta} = \frac{\boldsymbol{r}^{\mathbf{2}}}{\boldsymbol{R}} \tag{3}$$

where G is the shear modulus. Note that these equations are based on the assumption that r is much smaller than R to ensure a small deformation. From equations (2) and (3), the contact force F that can be used for haptic rendering is given by

$$F = \frac{8G\sqrt{R}}{3(1-\nu)}\delta^{3}/_{2} \tag{4}$$

Therefore, in the haptic rendering loop, given the indentation δ, the feedback force corresponding to the resulted deformation can be quickly calculated by this explicit representation.

Similarly, the contact force between a tool with a conical base and a plane, as shown in Fig. 2(b), can be derived as follows,

$$F = \frac{4G}{\pi(1-\nu)cot\alpha}\delta^{2} \tag{5}$$

where α is the conical angle.

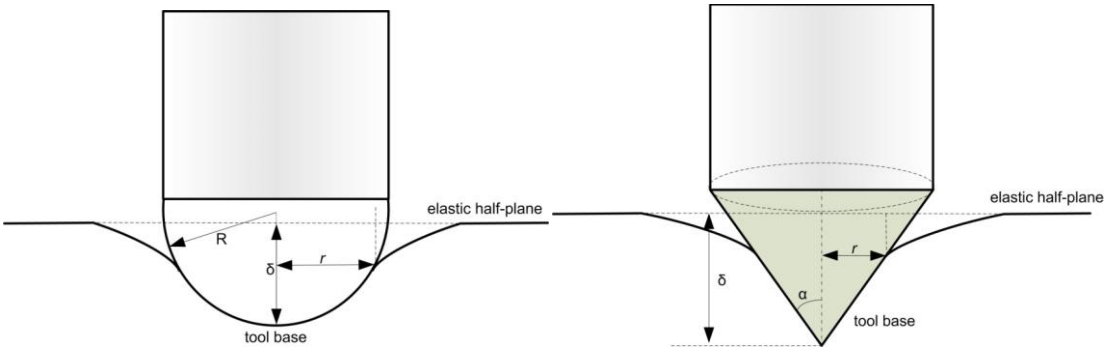

(a) spherical tool base (b) conical tool base

Fig. 2. Contact between two kinds of tool bases and an isotropic half plane.

3.2 **Validity of Assumption**

As the analytical force model assumes indentation into a planar surface, it is necessary to evaluate the validity of this assumption, i.e. the threshold that a curved surface can be regarded to be planar while the force discrepancy is not perceptible by the user in the simulation. Here, the physics-based FEM approach is adopted for the investigation. An experiment is conducted by comparing the indentation forces calculated by FEM at different object curvatures. Three spherical objects with radii R_0 of 30 mm, 50 mm and 100 mm are used respectively in the experiment, along with a cubic object with size of 100×100×50 mm^3 as the benchmark. Young's modulus and Poisson ratio are set to 50 kPa and 0.33 respectively. The

tool-tip is pushed perpendicularly towards the surface of the four objects respectively at a constant velocity. The FEM package ArtiSynth [28] is used to calculate the indentation forces. The forces are recorded at every 1 mm indentation into the object. Then, the force error e_f is calculated as,

$$e_f = \frac{F_s - F_c}{\max(F_c)} \times 100\% \quad (6)$$

where F_s is the force recorded with spherical objects and F_c with the cubic object. The force errors caused by indentation due to the spherical and conical bases of radius 10 mm are plotted respectively in Fig. 3. It is noted that when the indentation depth is small (below 9 mm for the spherical base (see Fig. 3(a)) and below 6.5 mm for the conical base (see Fig. 3(b))), the force errors for the three cubic objects with respect to the forces recorded with the cubic object are less than 7%, which is around the just-noticeable-difference (JND) of human force sensation [29]. That is, users are not able to feel the force differences due to mesh curvature within the ranges concerned in the experiment. In terms of feedback forces, the difference is not perceptible for small deformations even when the radius of the tool base (R=10 mm) is only three times smaller than that of the spherical object with R_0=30 mm, and the situation could be approximated by indentation into a plane.

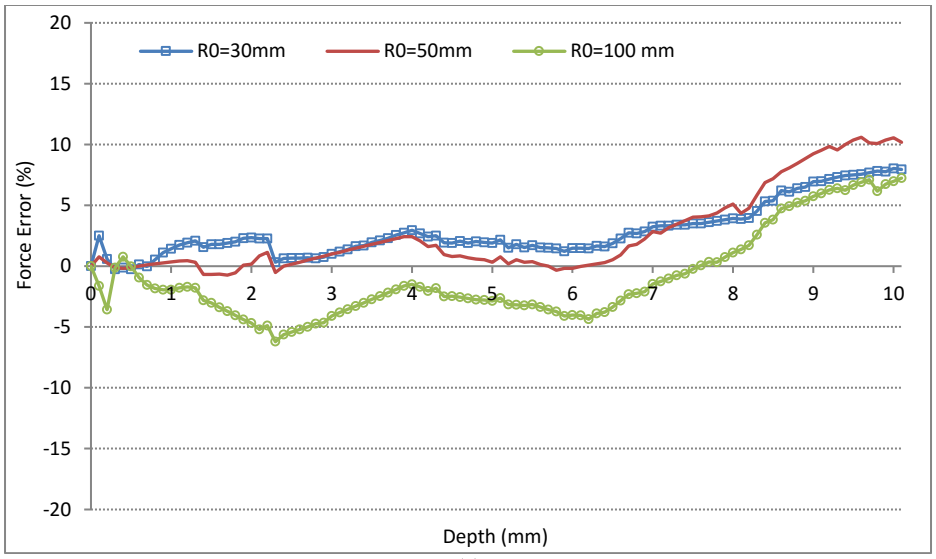

(a)

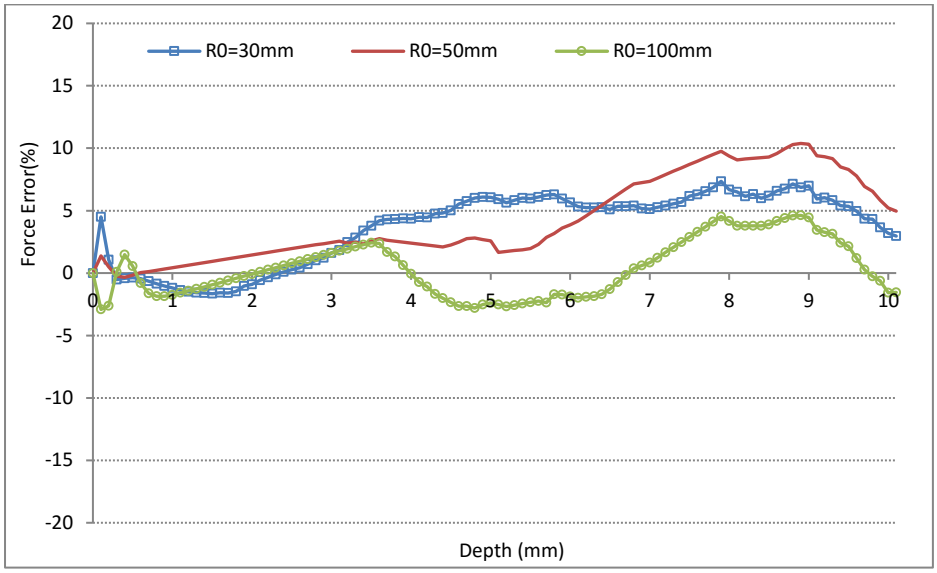

(b)

Fig. 3. Force error (max(F_c)=5.66 N) due to the approximation of curved surfaces as a plane: (a) spherical tool base, (b) conical tool base with α=45°.

In the proposed method, it is assumed in equation (1) that the indentation is perpendicular to the object's surface. However, in the simulation, the user can manipulate the tool to press the surface at some oblique angles. Consequently the assumption is no longer valid, especially for the tool with a conical base. Here, the JND of human force magnitude sensation (i.e. 7%) is used to evaluate the validity of the

assumption. For the tool with a spherical base, since the contact area remains circular upon inclination, the threshold inclination angle $\emptyset$ can be expressed analytically as

$$\emptyset = \operatorname{acos}\left(\frac{F_n}{F}\right) \leq \operatorname{acos}(1 - J_f) = \operatorname{acos}(1 - 0.07) \cong 22° \quad (7)$$

where F_n is the force perpendicular to the object surface, F is the force opposite to the indentation direction, and J_f is the JND of human force sensation. On the other hand, for a tool with a conical base, the contact area becomes elliptical upon inclination and the analytic equation is not valid. Therefore, FEM is used to obtain experimentally the forces at different inclinations and indentation depths, as the benchmark to compare with the forces calculated by the analytical model that assumes perpendicular contact. It is found that with JND = 7%, when the angle of the conical base is 45° and the indentation depth is less than 6 mm, the threshold inclination angle is 9°. Note that, as reported in [30], the discrimination threshold of force direction is about 32°, which is larger than the threshold angles obtained from equation (7) with the JND of force magnitude set to 7%. This means that a user would not feel any differences in both the force magnitudes and directions when the inclination angle is 22° for spherical base tool, or 9° for conical base tool, as if the tool were perpendicularly pressed against the surface of an object.

3.3 **Mesh Modeling**

In the proposed approach, mesh deformations are simulated efficiently in real time by geometrical modeling. The region of deformed surface is defined by the mesh points making contact with the tool base and the mesh, as shown by the mesh points denoted with open circles in Fig. 4. Here, the mesh is considered to be locally deformed and the deformed region is composed of two parts: the region Π in direct contact with the tool base and the surrounding region $\mho$. It is assumed that the deformed region has a circular boundary with radius R_d. $\mho$ and R_d are related to the mechanical properties of the object as well as the size and shape of the tool base. Hence, the deformed region is specified by the projection of the mesh points of the undeformed mesh onto the surface of the tool base (open circles) and $\mho$ (solid dots) respectively. Note that the mesh topology remains unchanged during the deformation. While the projection of mesh points onto Π is straightforward, the projection onto $\mho$ requires further deliberation.

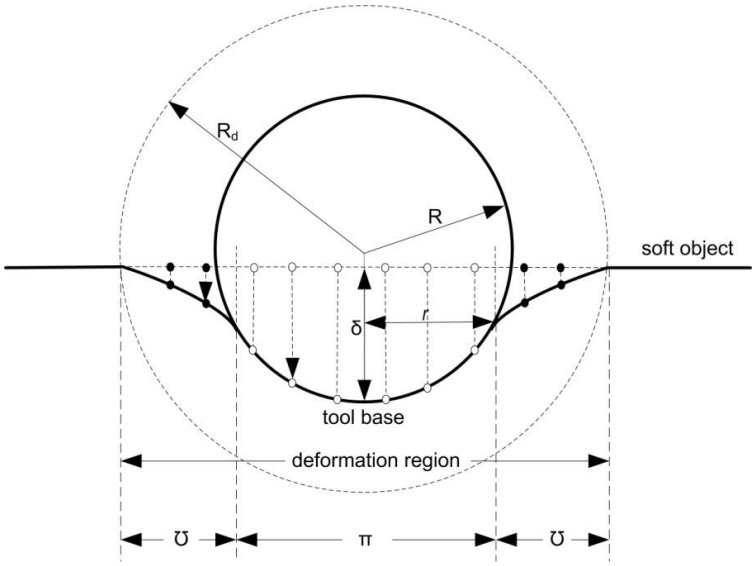

Fig. 4. Surface deformation model.

3.3.1 Projection onto ʊ

The region ʊ surrounding the contact area Π is represented by a series of Bézier patch surfaces which are defined by a set of control points $\boldsymbol{P}_{i,j}$ in space $\mathbb{R}^3$ as shown in Fig. 5(a). Bézier patch surfaces are used to represent the deformed surfaces herein since smooth deformed surfaces can be conveniently and efficiently represented by control points derived from the contact points. A patch surface, $\boldsymbol{S}(u, v)$, is defined by

$$\boldsymbol{S}(u,v) = \sum_{i=0}^{2}\sum_{j=0}^{1} B_i^2(u)B_j^1(v)\boldsymbol{P}_{i,j} \tag{8}$$

where the parameters u, v vary within [0, 1], $B_j^1(v)$ and $B_i^2(u)$ are the first-order and second-order Bernstein polynomials. Fig. 5(b) illustrates the determination of the control points based on the contact conditions. For example, when j=1, the control point $\boldsymbol{P}_{0,0}$ is the contact point between the tool base and the deformed mesh. This contact point is defined by the radius of the contact region. The control point $\boldsymbol{P}_{2,0}$ is determined by the radius R_d of the deformed region. The line L_1 is tangential to the undeformed surface and passes through the point $\boldsymbol{P}_{2,0}$. The line L_2 is tangential to the contact surface at point $\boldsymbol{P}_{0,0}$. Then, the third control point $\boldsymbol{P}_{1,0}$ is obtained by calculating the intersection between L_1 and L_2. After obtaining these

control points, the corresponding Béizer surface can be determined by equation (8). When all the patch surfaces constituting υ are obtained, tessellation is applied to convert them into triangular meshes [31]. Finally, the mesh points of the undeformed mesh are projected onto these triangles to yield the deformed mesh.

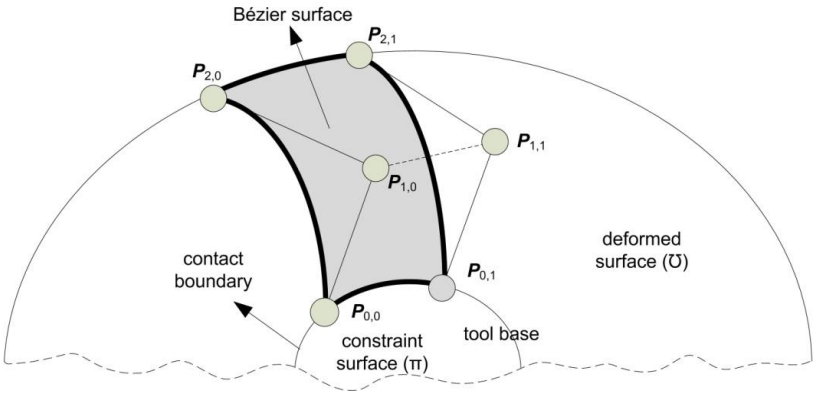

(a)

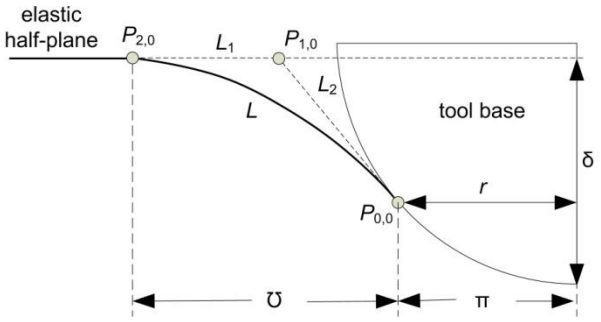

(b)

Fig. 5. Modeling of deformed meshes: (a) top view, (b) side view.

3.3.2 FEM Calibration

As the proposed mesh deformation approach is based on the geometric modeling, it is necessary to ensure the non-physics based simulation is able to replicate deformations in a realistic manner. To achieve this, FEM is first used to obtain the relationship between indentation and the deformation extent. The pre-computed results then serve as a "lookup table" to define the deformation of geometrical mesh in real time. The lookup table gives the relation between insertion depth (δ) and deformation size defined by R_d, which is used in the mesh modeling based on Bézier patch surfaces. Since the indentation depth is not large (small

deformation), for a spherical base tool with a radius R=10 mm and a maximum indentation depth of 10 mm, deformation is computed at a step size of 0.5mm for 20 steps, i.e. equidistantly sampled. That is, the lookup table is a table with 2 columns (δ and R_d) and 20 rows. For a given indentation depth, the table is accessed to obtain the corresponding value R_d which is used to locally update the deformed region of the mesh. Hence, graphics rendering can be performed very quickly.

Using ArtiSynth, the FEM simulation is conducted by vertically indenting (i.e. along negative Z-axis in Fig. 6) against a rectangular object with size of 100×100×50 mm^3 by a tool with a spherical (R=10 mm) and conical base (R=10 mm, α=45°) respectively. The scenario of indentation using a spherical tool base is shown in Fig. 6. An indentation of 10 mm is made in the experiment. The deformed region is thus circular with a radius R_d when viewed from the top, and is defined by the region where the surface is depressed by more than 0.5 mm. In other words, the undeformed regions refer to the regions where the surface is depressed by less than 0.5 mm. In the experiment, Young's modulus of the rectangular object is set to 50 kPa and 1.5 MPa respectively, and Poisson's ratio is 0.33. The lateral views of the deformation region at different depths are shown in Fig. 7. As the tool base is pushed vertically down, the deformed region grows as shown in Fig. 7(a)~(d). Since the contact area of the conical base tool is relatively small, the size of the deformed region is small as well (Fig. 7(c) and (d)) when compared with that of the spherical base tool (Fig. 7(a) and (b)).

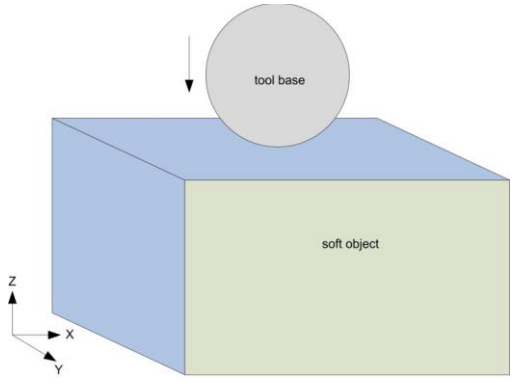

Fig. 6. Setting of the FEM calibration experiment.

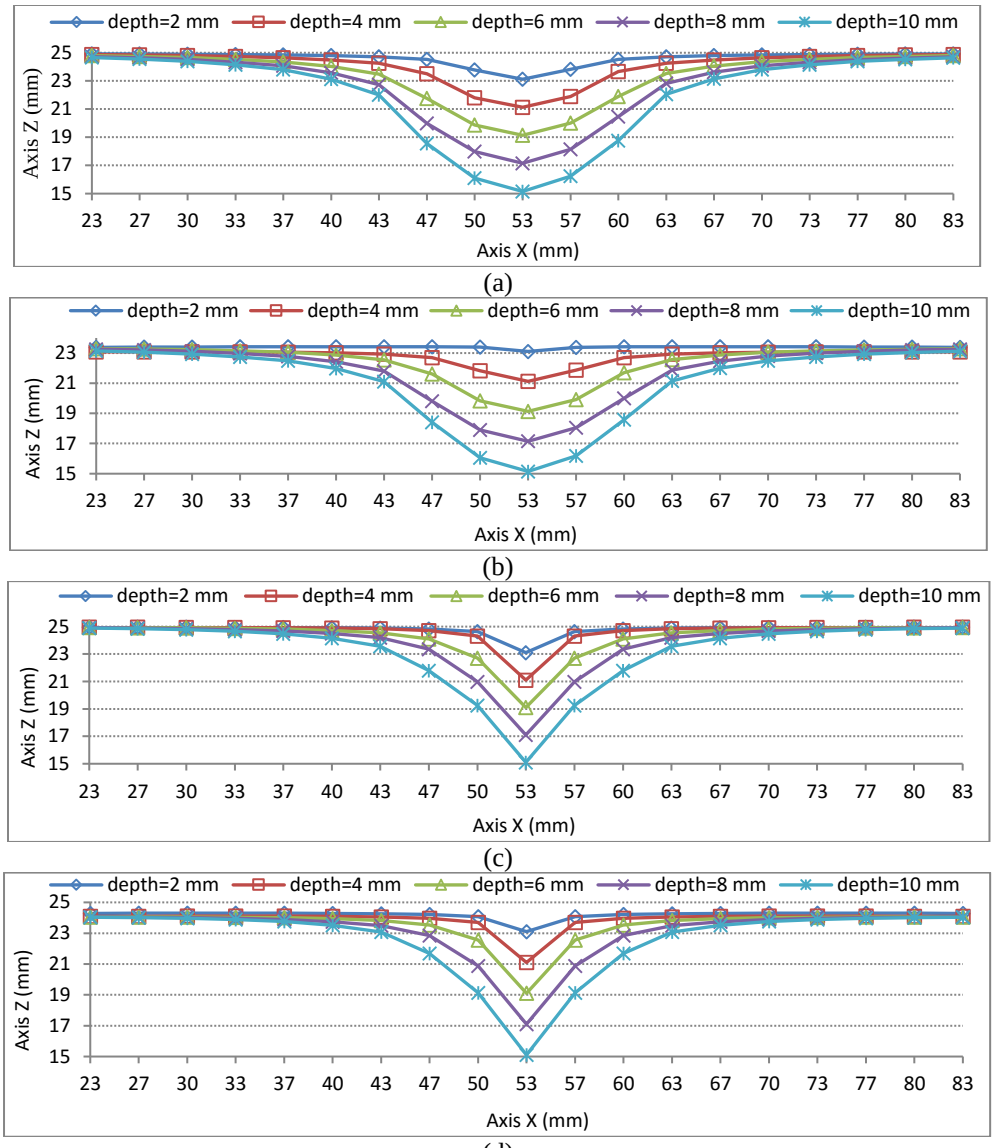

Fig. 7. Surface deformation profiles obtained by the FEM simulation with different indentation depths and material elasticity. In (a) and (b), a spherical tool base with R=10 mm is depressed against an object with Young's modulus 1.5 MPa and 50 kPa respectively. In (c) and (d), a conical tool base with R=10 mm and α=45° is depressed against an object with Young's modulus 1.5 MPa and 50 kPa respectively. In all cases, Poisson ratio is 0.33.

Furthermore, the variation of R_d with indentation depth δ is studied for the spherical tool base with R=10 mm as shown in Fig. **8**(a). For small indentation (say, less than around 7 mm), the relationship between R_d and δ can be approximated simply by a linear function. To cater for larger indentation, the experimental data can be fit to a quadratic function to estimate the radius of the deformed region for a wider range of indentation depth. The corresponding graph for the conical tool base is shown in Fig. **8**(b). For the conical tool base, since the contact area between the tool base and object's surface is smaller when compared with that of spherical tool base, the deformed region caused by the conical base has a smaller R_d. By using the obtained relationship between the size of deformed region and indentation depth, the mesh shape can be changed based on the aforementioned approach to visually render the object in a manner close to the deformation calculated by the physics-based FEM but at a fast speed.

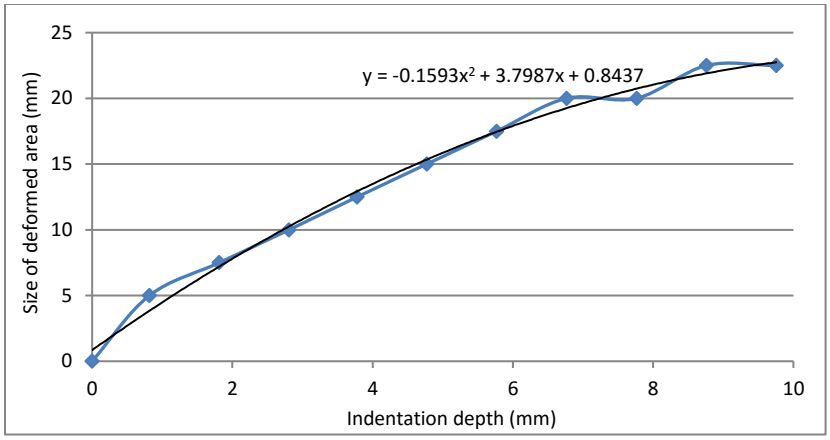

(a)

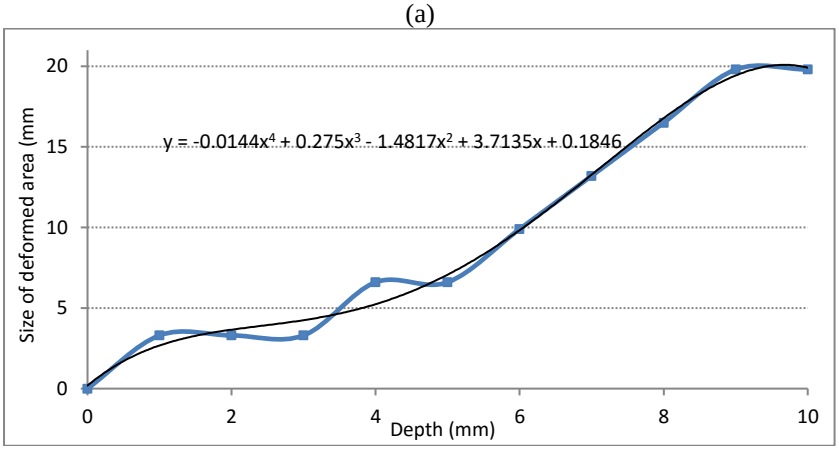

(b)

Fig. 8. Radius R_d of the deformation region at different indentation depths using (a) spherical and (b) conical tool base respectively, both with R=10 mm.

4. Experiments

In this section, the proposed method is used to implement an interactive medical simulation system with haptic feedback. The system is presented in Section 4.1. The goal of evaluating the two types of tools is to verify that the proposed model can achieve good computation efficiency while accomplishing satisfactory force accuracy. The computational speed and model accuracy of the system are evaluated in Section 4.2 and Section 4.3 respectively, with reference to the assessment framework for medical simulation system in [32].

4.1 Simulation System

The framework of the interactive medical simulation system is illustrated in Fig. 9(a). It contains dedicated modules for 3D graphic rendering, collision detection, mesh deformation, and analytical force calculation. The haptic rendering pipeline is further elaborated with Fig. 9 (b), where the indentation depth is obtained to calculate the response forces using the analytical force model, followed by the application of damping force before driving the haptic device. The experiment is conducted using a virtual liver model and tools with spherical and conical bases, as shown in Fig. 10. For the liver model, mesh with two levels of details is employed, where the fine mesh is used for visual display and the less detailed mesh for haptic rendering. The simulation system is implemented on a personal computer equipped with an Intel® Core™ i7-2600 (3.4G Hz) processor, 4 GB RAM and an NVIDIA Quadro 4000 graphics display card. The operation system is Windows 7 Enterprise (32 bits). The PHANTOM® Desktop™ haptic device (manufactured by the Sensable Technologies) is used to provide 6 degree-of-freedom positional input and 3 degree-of-freedom force output as shown in Fig. 11.

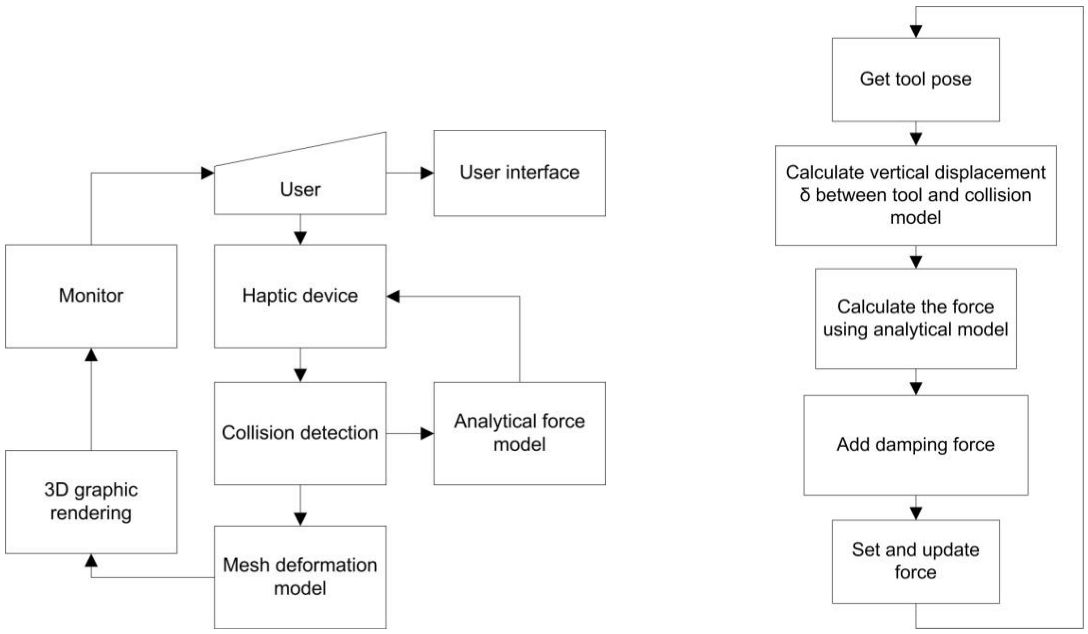

(a) (b)

Fig. 9. Bock diagrams of the system workflow.

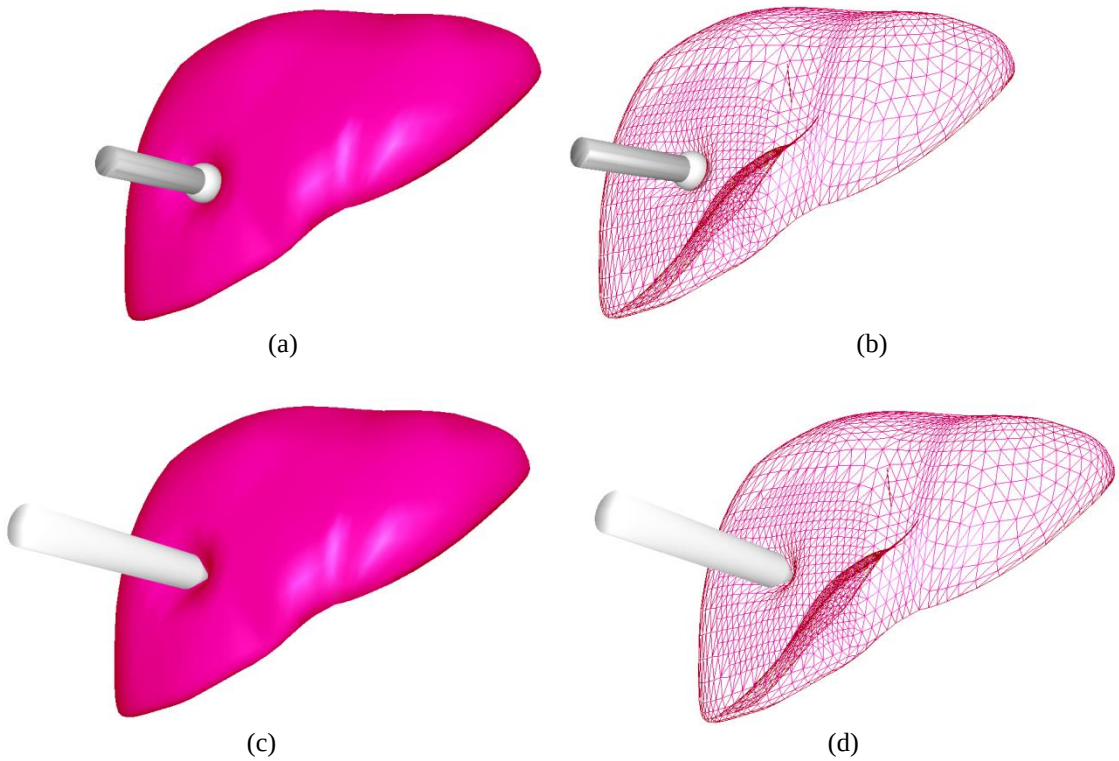

Fig. 10. Interactive deformations of a liver model using the analytical force model: the liver model is depressed by a tool with a spherical base in (a) and (b), and by another tool with a conical base in (c) and (d).

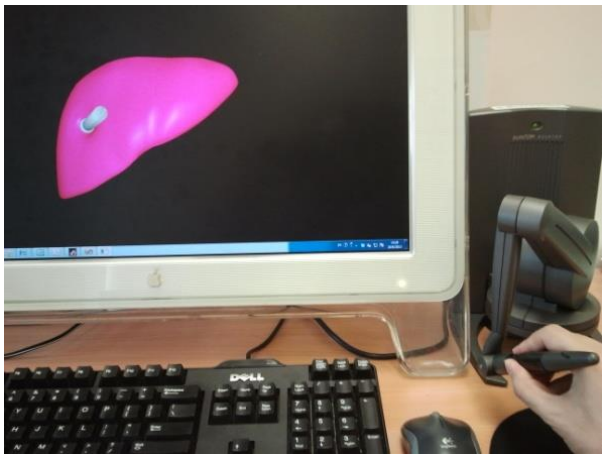

Fig. 11. The haptic device used in the experimental system.

To increase computational speed, a two-phase collision detection approach is implemented for collision detection, namely, broad and narrow phases. In the broad phase, bounding-box hierarchy is employed to determine if the surface mesh of the liver model potentially intersects with the tool. If

intersection occurs, the broad phase collision detection algorithm returns the pairs of colliding bounding volumes (axis-aligned bounding boxes). The narrow phase detection is then invoked to check whether the mesh points bounded by the returned bounding boxes are within the tool base. The computation in this phase is fast since the tool base is represented by an implicit function. The contact normal is calculated by averaging the normal vector at all the colliding points. The vertical displacement δ is calculated based on the center of the contact points and the proximal end of the tool base along the contact normal. The two-phase detection method enables the mesh to be updated by the deformation model in the graphic rendering loop running at about 50 Hz. And at the same time, feedback force is calculated in the haptic servo loop running at 1 kHz, as shown in Fig. 9(b). Snapshots of the interactions between the elastic liver model and the tool with a spherical base are shown in Fig. 10(a) and (b). Snapshots for the tool with a conical base are shown in Fig. 10(c) and (d).

4.2 **Timing Performance**

In addition, experiments are conducted to evaluate the computational efficiency of the proposed method. A surface model with 1600 vertices, 4641 edges and 3042 triangles is created, which is depressed by a tool with a spherical base of radius 10 mm. The computation time per step recorded during the interactions is shown in Fig. 12(a). By using the analytical force model and the FEM-calibrated geometric mesh deformation, it is found that computation time required at each time step is well within 0.25 ms (4 kHz) and can be completed in the haptic servo loop. This demonstrates that the proposed approach is suitable for real-time interactive simulation of both haptic and visual feedbacks for deformable objects. The timing performance is also compared with that of FEM and MSS simulations. In the comparison, the Simulation Open Framework Architecture (SOFA) [33] is adopted. It is an open source framework developed for real-time interactive medical simulation. The computation time of FEM and MSS is measured under the same experimental conditions as that for evaluating the proposed method – all the three models are executed on the same machine with the same surface models. In the simulation, the backward Euler scheme is used for implicit time integration, and the conjugate gradient iterative algorithm is employed as the linear system solver. It is found that it takes about 20 ms for FEM (Fig. 12(b)) and 15 ms for MSS (Fig. 12(c).) to complete one step of deformation simulation. The FEM and MSS models can only

be performed in the graphics loop at about 50 Hz, and they cannot be directly run in the 1 kHz haptic servo loop.

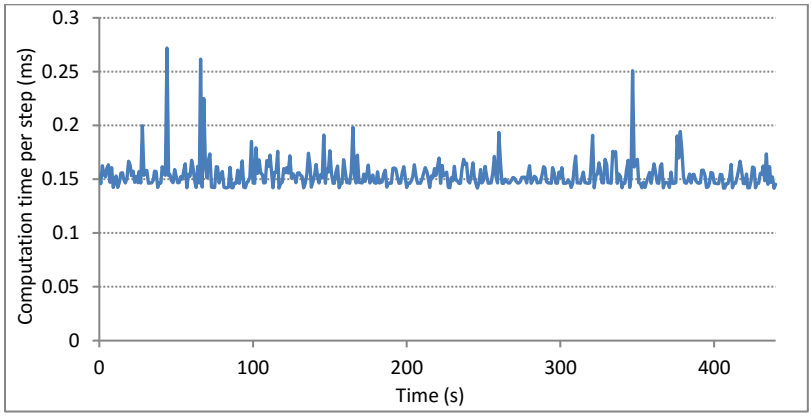

(a) Computation performance of the analytical force model

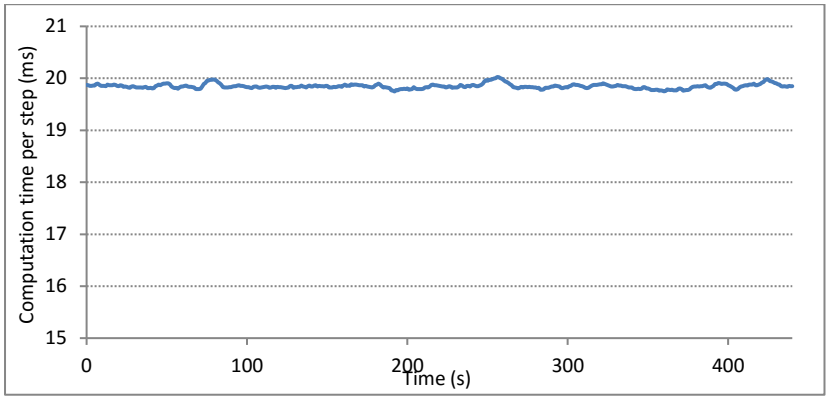

(b) Computation performance of the FEM model

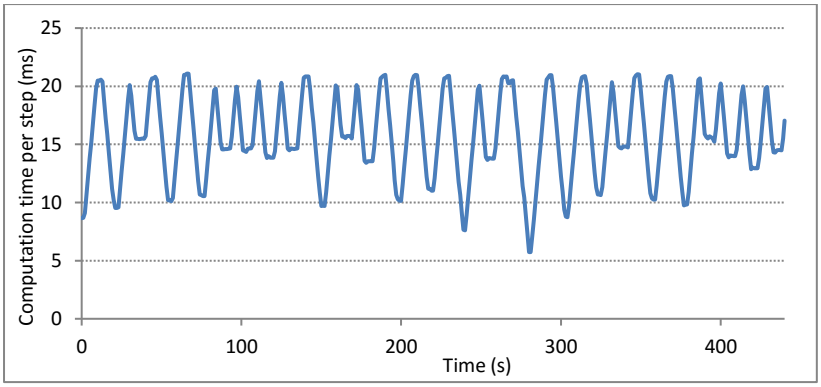

(c) Computation performance of the MSS model

Fig. 12. Computation performance of the three simulation methods on a surface model with 1600 vertices, 4641 edges and 3042 triangles.

To further investigate the computation efficiency of the proposed analytical force model, a surface model with higher spatial resolution is employed in the experiment, which contains 10000 vertices, 29601 edges and 19602 triangles. The time spent on the haptic rendering loop is shown in Fig. 13. It can be seen that forces can still be directly and stably rendered at 1 kHz refresh rate for this high resolution surface model.

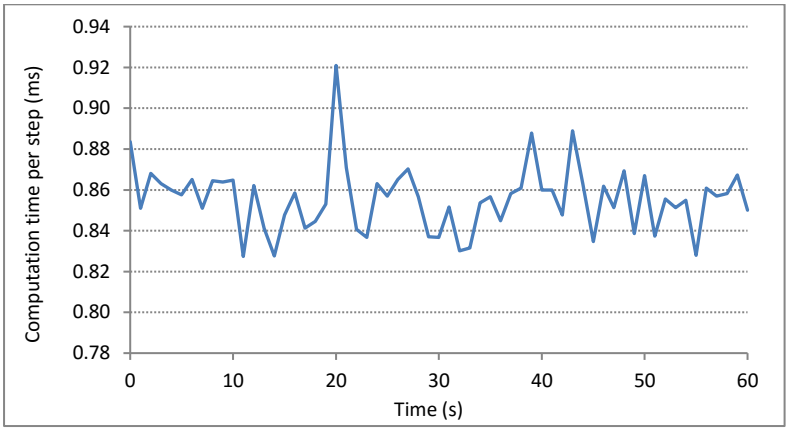

Fig. 13. Computation performance of the analytical force method on a surface model with 10000 vertices, 29601 edges and 19602 triangles.

In addition to the aforementioned models, other models with different resolution are evaluated by experiments similar to the work in [34]. The results are listed in Table 1. As the mesh resolution increases, the computation time per step grows proportionally. From Fig. 14, it can be seen there is a linear relationship between the mesh complexity and average computation time per step.

Table 1. The relationship between computation time per step (millisecond) and mesh complexity.

Model	Mesh Complexity			Computation Time per step (ms)	
	Vertex	Edge	Triangle	Mean	SD
1	1600	4641	3042	0.154	0.014
2	2500	7301	4802	0.231	0.012
3	3600	10561	6962	0.325	0.014
4	4900	14421	9522	0.426	0.013
5	6400	18881	12482	0.551	0.012
6	8100	23941	15482	0.696	0.025
7	10000	29601	19602	0.856	0.016

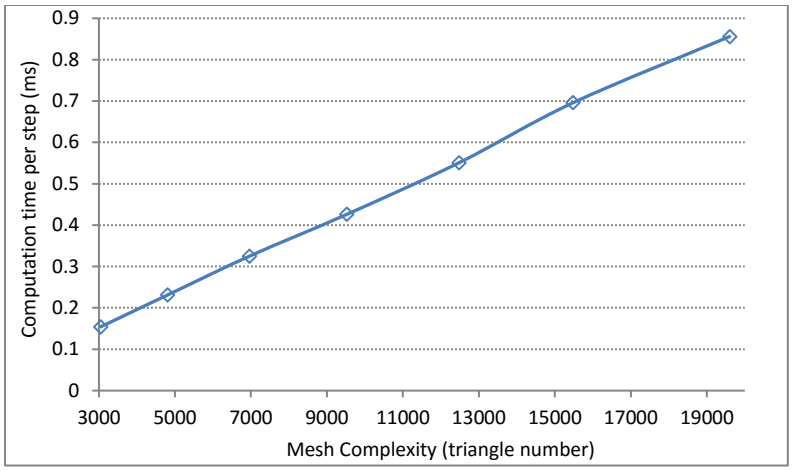

Fig. 14. Average computation time versus mesh complexity.

4.3 **Feedback Force Accuracy**

Furthermore, an experiment is conducted to investigate the accuracy of feedback forces computed using the analytical force model by comparing that of FEM [35]. In the comparisons, a volumetric mesh of 100×100×30 mm^3 (30×30×10 nodes) is created. Young's modulus and Poisson ration are 50 kPa and 0.33 respectively. Tools with a spherical base of radius 6 mm and a conical base with α=45° are used to indent the volumetric mesh. Here, FEM is used to simulate the feedback forces arising from interactions with both linear and neo-Hookean materials. The latter is adopted in the comparison to investigate the model's applicability for surgical simulation which concerns human tissues that are nonlinear in general. Constrained backward Euler integrator is used to solve the FEM equations. The variations in contact force with indention depth as recorded by using the proposed approach to simulate linear material, and by using FEM to simulate linear and neo-Hookean materials are shown in Fig. 15. The force calculated by the analytical force model is close to that of the linear FEM model when the depth is less than 6 mm, and becomes larger when the indentation depth further increases as shown in Fig. 15(a) for the case of the spherical base. When compared with the force calculated by FEM on neo-Hookean materials, both the proposed approach and linear FEM model underestimate the feedback forces, and the discrepancy increases with indentation depth. As for the case of the conical base (Fig. 15(b)), the forces generated by the analytical force model are relatively smaller than that of linear and neo-Hookean material models. When the depth is less than 2.5 mm, the forces of the analytical force model and the linear material model are

almost equal. Beyond that, the forces calculated by the analytical force model are smaller than the forces calculated for the neo-Hookean material but greater than that for linear FEM model.

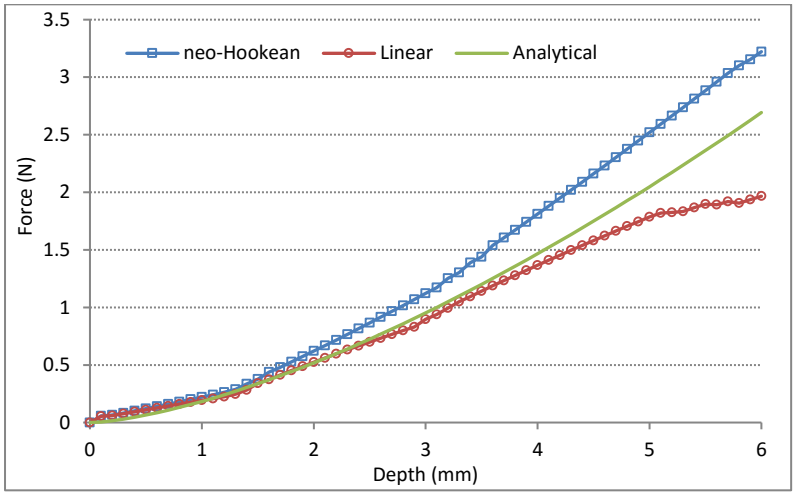

(a) spherical base case (R=6 mm)

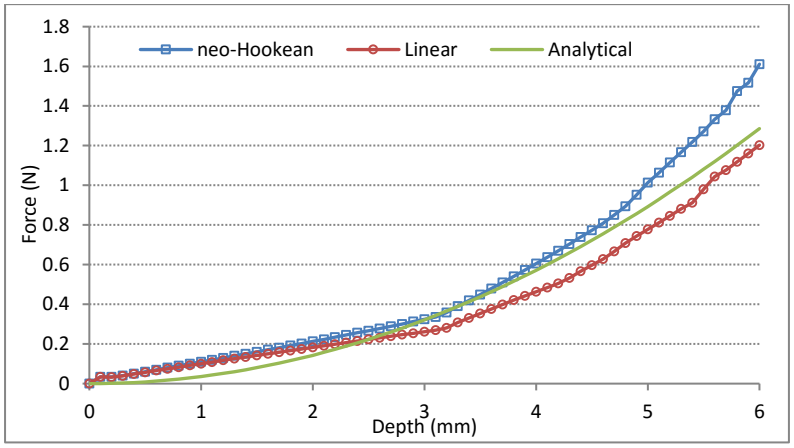

(b) conical base (R=6 mm, α=45°)

Fig. 15. Variation of feedback forces with indentation depth using different force models.

The small deformation constraint is also investigated by analyzing the results from the aforementioned experiments. Fig. 16 shows the force difference between the proposed analytical model and the FEM method for linear and non-linear materials. The force difference (e_f) is calculated as

$$e_f = |f_a - f_f| \times 100/f_m \quad (9)$$

where f_a is the force calculated by the analytical model, f_f is the force generated by FEM with linear or non-linear materials, $|\cdot|$ is the absolute value operator, f_m is the maximum force in the experiment**.** If the force difference is under 7% which is around the JND of human force sensation [29], then, the depth (δ) could be as large as 3.3 mm for neo-Hookean material. For the linear material, the depth constraint could be relaxed to as large as 4.3 mm.

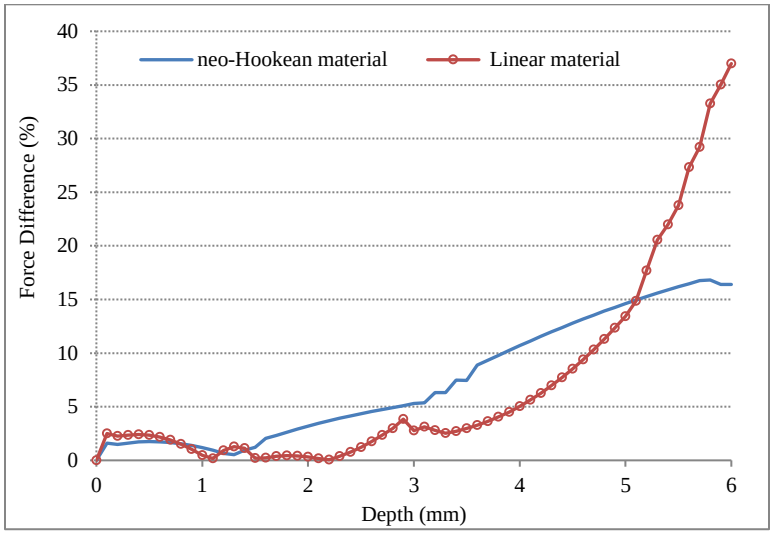

Fig. 16. Plot of force difference between the analytical force model and FEM with linear and non-linear materials for the tool with a spherical base.

5. Discussions

While the proposed analytical force model has demonstrated computational efficiency for the simulation of soft objects, special consideration are required to determine the conditions where the model is applicable. First, the proposed approach assumes that contacts are made with a plane or deformable object with small curvature. It is applicable to scenarios where the curvature of the object is comparable to that of the tool base. When contact is made on an object at a region with steep curvatures, one possible approach is to approximate the contact region locally with a parametric surface where an analytical force model similar to the one proposed can be developed to obtain the relationship between the applied forces and deformation [27]. The deformation result is then reflected back onto the object via a mapping mechanism. Besides, although mesh deformations are FEM-calibrated, the proposed approach only takes surface deformations into account. Unlike other physical models, it does not model volume changes due to deformations.

Indentation in one place will not cause inflation or bulge in other places. Hence, the approach is applicable to small deformations, for examples, in situations where the size of soft object is much larger than the deformation region, or the object is bulky with small curvature. To ensure small deformations as required by the assumption of linear elasticity, the object stiffness shall be large enough so that the indentation forces are rendered within a reasonable range. Otherwise, if the stiffness is small (i.e., the object is too soft), users are limited to apply small forces. However, it is found in the experiment (Section 4.3) that the constraint could be relaxed to such an extent that the depth could be comparable to the tool size. Therefore, the proposed force model could be employed to simulation scenarios where a tool with a large tip size is used.

Furthermore, the shape of the deformed zone is regarded as a circular area on the object's surface. This assumption may not be valid when the tool interacts with an object with complex geometry. It is indeed found that the size of the deformed zone is related to boundary conditions. Therefore, a more robust model that takes boundary conditions into account is required, in addition to the shape and size of the tool base and physical properties of the deformable object.

The analytical force model described in equation (1) is a general formula that expresses indentation force with respect to tool size, shape and physical properties of soft deformable object. In this study, tools with spherical and conical bases are considered, and the two force models derived assume small deformations. It is shown in the experiments that when indentation is small, the behavior of the analytical force model is similar to those of the hyper-elastic and linear materials (see Fig. 15). Analytical force models for other types of tool bases can be obtained in the same way. As for indentation direction, we have analyzed the validity of inclination indentation for the two types of tools in Section 3.2. However, it is also possible to develop a more general force model that takes into account the indentation direction.

In the proposed method, since the surface deformation model is decoupled from the force model, it is straightforward to use different geometric models for graphics and haptic rendering. In the proposed approach, a fine geometric model is used for graphic rendering and a coarse model for haptic rendering. This is similar to multi-model strategies commonly used in FEM simulation [33], where a mapping

mechanism is applied to reflect the deformation results obtained from the physical model to the visual model. In contrast, the two models are decoupled in the proposed approach.

In addition to using Bézier surfaces to model the deformed surface, B-spline surfaces and surface subdivision may also be adopted to produce smoother surfaces and better visual effect. However, in the surface representation model of the proposed method, since the control points are obtained only based on contact conditions and offline simulation results (i.e. deformation size defined by Rd), the definition of the knot vectors for B-spline is unclear. On the other hand, an issue with surface subdivision is the choice of suitable subdivision scheme that is able to physically represent the deformed surfaces. Besides, for real-time interactive applications, it is also necessary to deal with the computational overhead of surface subdivision.

Note that the accuracy of feedback force calculation of the proposed method is not compared with that of MSS. It is because the parameters in MSS are usually tuned by some heuristic methods based on the experimentally measured data or the simulation results of more accurate physical models, e.g. FEM [36]. Furthermore, it was also claimed that linear elastic material cannot be approximated by MSS with homogeneous parameters [37]. That is, the accuracy of MSS is dependent on the settings of model parameters, which is vague and make it impracticable to perform a fair comparison.

Future work will be conducted to employ the approach for the simulation of medical palpation, e.g. liver diagnosis [38]. We aim to develop a palpation simulator for abdominal examination with haptic feedback using the proposed analytical force model. The 3D model of human abdomen will be obtained from MRI image data. In view of the fact that the tissues are inhomogeneous and anisotropic, layered deformation model based on the proposed analytical force model is to be developed, where efficient and realistic force rendering are anticipated. Trainees will feel the shapes of the internal organs with the simulator.

6. Conclusions

In this paper, an analytical force model is proposed as an alternative soft-object deformation simulation approach. The model is derived from contact theory based on elastic mechanics. Experimental results show that forces rendered by the proposed approach are comparable to that calculated by FEM. One evident advantage of this approach is the computational efficiency that makes it possible to execute the algorithms directly in a haptic servo loop at 1 kHz refresh rate. While mesh deformations are modeled geometrically and surface deformations are only considered, it is calibrated with FEM to simulate the effect of indentation depth on the size of deformation region. The offline pre-computed FEM data serve as a benchmark to update the shapes of Bézier surfaces in real time according to the contact conditions. This ensures that the surface mesh is deformed and visualized in a physically realistic manner. The approach is easy to be implemented, computationally efficient and provides reasonable physical fidelity. It is thus a promising approach for many real-time interactive applications.

Acknowledgments

This work was supported in part by the Research Grants Council of Hong Kong SAR (Project No. PolyU 5134/12E, 5152/09E) and the Hong Kong Polytechnic University (Project Account Code 87RF).

References

1. Pai DK, Doel K, James DL, Lang J, Lloyd JE, Richmond JL, Yau SH (2001) Scanning physical interaction behavior of 3D objects. In: Proceedings of the 28th annual conference on Computer graphics and interactive techniques, 2001. ACM, pp 87-96
2. Meier U, Lopez O, Monserrat C, Juan M, Alcaniz M (2005) Real-time deformable models for surgery simulation: a survey. Computer methods and programs in biomedicine 77 (3):183-197
3. Luciano CJ, Banerjee PP, Rizzi SHR (2007) GPU-based elastic-object deformation for enhancement of existing haptic applications. In: IEEE International Conference on Automation Science and Engineering, 2007. IEEE, pp 146-151
4. Wang P, Becker A, Jones I, Glover A, Benford S, Greenhalgh C, Vloeberghs M (2007) Virtual reality simulation of surgery with haptic feedback based on the boundary element method. Computers & structures 85 (7):331-339
5. Mafi R, Sirouspour S, Mahdavikhah B, Moody B, Elizeh K, Kinsman A, Nicolici N (2010) A parallel computing platform for real-time haptic interaction with deformable bodies. IEEE Transactions on Haptics 3 (3):211-223
6. Nealen A, Müller M, Keiser R, Boxerman E, Carlson M (2006) Physically based deformable models in computer graphics. In: Computer Graphics Forum, 2006. Wiley Online Library, pp 809-836
7. Terzopoulos D, Platt J, Barr A, Fleischer K (1987) Elastically deformable models. In: ACM Siggraph Computer Graphics, 1987. ACM, pp 205-214
8. Sederberg TW, Zheng J, Bakenov A, Nasri A (2003) T-splines and T-NURCCs. In: ACM Transactions on Graphics (TOG), 2003. ACM, pp 477-484
9. Sederberg TW, Parry SR (1986) Free-form deformation of solid geometric models. In: ACM Siggraph Computer Graphics, 1986. ACM, pp 151-160
10. Milliron T, Jensen RJ, Barzel R, Finkelstein A (2002) A framework for geometric warps and deformations. ACM Transactions on Graphics (TOG) 21 (1):20-51
11. Abdelrahman W (2012) Towards an efficient haptic rendering using data-driven modeling. Deakin University, Melbourne

12. Duysak A, Zhang JJ, Ilankovan V (2003) Efficient modelling and simulation of soft tissue deformation using mass-spring systems. In: International Congress Series, 2003. Elsevier, pp 337-342
13. Zilles CB, Salisbury JK (1995) A constraint-based god-object method for haptic display. In, IEE/RSJ International Conference on Intelligent Robots and Systems, Human Robot Interaction, and Cooperative Robots, 1995. IEEE, pp 146-151
14. Ruspini DC, Kolarov K, Khatib O (1997) The haptic display of complex graphical environments. In: Proceedings of the 24th annual conference on Computer graphics and interactive techniques, 1997. ACM Press/Addison-Wesley Publishing Co., pp 345-352
15. Colgate JE, Stanley MC, Brown JM (1995) Issues in the haptic display of tool use. In: Intelligent Robots and Systems 95.'Human Robot Interaction and Cooperative Robots', Proceedings. 1995 IEEE/RSJ International Conference on, 1995. IEEE, pp 140-145
16. Hasegawa S, Ishii M, Koike Y, Sato M (1999) Inter-process communication for force display of dynamic virtual world. ASME DYN SYST CONTROL DIV PUBL DSC 67:211-218
17. McNeely WA, Puterbaugh KD, Troy JJ (1999) Six degree-of-freedom haptic rendering using voxel sampling. In: ACM SIGGRAPH 1999, 1999. ACM, pp 401-408
18. Moustakas K, Tzovaras D, Strintzis MG (2007) SQ-Map: Efficient layered collision detection and haptic rendering. IEEE Transactions on Visualization and Computer Graphics 13 (1):80-93
19. Courtecuisse H, Jung H, Allard J, Duriez C, Lee DY, Cotin S (2010) GPU-based real-time soft tissue deformation with cutting and haptic feedback. Progress in biophysics and molecular biology 103 (2):159-168
20. Delingette H (2008) Biquadratic and Quadratic Springs for Modeling St Venant Kirchhoff Materials. Biomedical Simulation:40-48
21. Bro-Nielsen M, Cotin S (1996) Real-time Volumetric Deformable Models for Surgery Simulation using Finite Elements and Condensation. In: Computer graphics forum, 1996. Wiley Online Library, pp 57-66
22. Felippa CA (2000) A systematic approach to the element-independent corotational dynamics of finite elements. Center for Aerospace Structures, College of Engineering, University of Colorado, Boulder
23. Comas O, Taylor Z, Allard J, Ourselin S, Cotin S, Passenger J (2008) Efficient nonlinear FEM for soft tissue modelling and its GPU implementation within the open source framework SOFA. Biomedical Simulation:28-39
24. Courtecuisse H, Cotin S, Allard J, Soler L (2011) GPU-based interactive simulation of liver resection. In: ACM SIGGRAPH 2011 Computer Animation Festival, 2011. ACM, pp 98-98
25. Fong P (2009) Sensing, acquisition, and interactive playback of data-based models for elastic deformable objects. The International Journal of Robotics Research 28 (5):630-655
26. Deo D, De S (2009) PhyNeSS: A Physics-driven Neural Networks-based Surgery Simulation system with force feedback. In: EuroHaptics conference, 2009 and Symposium on Haptic Interfaces for Virtual Environment and Teleoperator Systems. World Haptics 2009. Third Joint. IEEE, 2009. IEEE, pp 30-34
27. Kachanov ML, Shafiro B, Tsukrov I (2003) Handbook of elasticity solutions. Springer, Dordrecht, The Netherlands
28. Lloyd JE, Stavness I, Fels S (2012) ARTISYNTH: A fast interactive biomechanical modeling toolkit combining multibody and finite element simulation. Soft Tissue Biomechanical Modeling for Computer Assisted Surgery:355-394
29. Pang XD, Tan HZ, Durlach NI (1991) Manual discrimination of force using active finger motion. Attention, Perception, & Psychophysics 49 (6):531-540
30. Yang X-D, Bischof WF, Boulanger P (2008) The effects of hand motion on haptic perception of force direction. In: Haptics: Perception, Devices and Scenarios. Springer, pp 355-360
31. Piegl LA, Tiller W (1998) Geometry-based triangulation of trimmed NURBS surfaces. Computer-Aided Design 30 (1):11-18
32. Marchal M, Allard J, Duriez C, Cotin S (2008) Towards a framework for assessing deformable models in medical simulation. In: Biomedical Simulation. Springer, pp 176-184
33. Allard J, Cotin S, Faure F, Bensoussan PJ, Poyer F, Duriez C, Delingette H, Grisoni L (2007) SOFA-an open source framework for medical simulation. In: Medicine Meets Virtual Reality, MMVR 15, 2007. pp 13-18
34. Ullrich S, Rausch D, Kuhlen T (2011) Bimanual haptic simulator for medical training: system architecture and performance measurements. In: Proceedings of the 17th Eurographics conference on Virtual Environments & Third Joint Virtual Reality, 2011. Eurographics Association, pp 39-46
35. Alterovitz R, Goldberg K (2002) Comparing algorithms for soft tissue deformation: accuracy metrics and benchmarks. Rapport technique, UC Berkeley: Alpha Lab:42-44
36. Natsupakpong S, Cenk Çavuşoğlu M (2010) Determination of elasticity parameters in lumped element (mass-spring) models of deformable objects. Graphical Models 72 (6):61-73
37. Bianchi G, Solenthaler B, Székely G, Harders M (2004) Simultaneous topology and stiffness identification for mass-spring models based on FEM reference deformations. In: Medical Image Computing and Computer-Assisted Intervention–MICCAI 2004. Springer, pp 293-301
38. Hamza-Lup FG, Bogdan CM, Seitan A (2012) Haptic simulator for liver diagnostics through palpation. Studies in Health Technology and Informatics 173:156-160